ACOUSTICS 2012

On the use of a SAFE-PML technique for modeling two-dimensional open elastic waveguides

F. Treyssede[a], K.-L. Nguyen[a], A.-S. Bonnet-Bendhia[b] and C. Hazard[b]

[a]IFSTTAR-MACS, Route de Bouaye, CS4, 44344 Bouguenais Cedex, France
[b]ENSTA-UMA, POEMS (UMR7231), 32, Boulevard Victor, 75739 Paris Cedex 15, France
fabien.treyssede@ifsttar.fr

Elastic guided waves are of interest for inspecting structures due to their ability to propagate over long distances. However, when the guiding structure is embedded into a solid matrix, usually considered as unbounded, waveguides are open and waves can be trapped or leaky. In the latter case, the leakage of energy into the surrounding medium yields attenuation along the axis of the waveguide, which can strongly limit the application of guided wave techniques. Analytical tools have been developed for studying open waveguides but they are limited to simple geometries (plates, cylinders). With numerical methods, one of the difficulties is that leaky modes, which attenuate along the axis (complex wavenumber), grow exponentially along the transverse directions. A simple procedure used with existing codes consists in using absorbing layers of artificially growing viscoelasticity, but large layers are often required. The goal of this work is to propose a numerical approach for computing modes in open elastic waveguides combining the so-called semi-analytical finite element method and a perfectly matched layer technique. Two-dimensional problems are considered. Numerical solutions are compared to analytical results. The efficiency of both perfectly matched and absorbing layer techniques is evaluated.

1 Introduction

Elastic guided waves are of interest for inspecting structures due to their ability to propagate over long distances. In several applications, the elastic waveguide, invariant along its axis, is embedded in another solid matrix. When the guiding structure is surrounded by another medium, usually considered as unbounded, waveguides are open and waves can be trapped or leaky. In the latter case, the leakage of energy into the surrounding medium yields attenuation along the axis of the waveguide. Owing to these radiation losses, the axial wavenumber becomes complex. Such losses can strongly limit the application of guided wave techniques.

When the velocity of shear waves in the waveguide is greater than in the surrounding medium, no trapped modes are present and only leaky modes occur [1]. Such a configuration is widely encountered in civil engineering applications, the embedding medium usually consisting of soft materials (e.g. cement, concrete, soil). An accurate determination of leaky modes appears to be a necessary step for nondestructive evaluation (NDE) of embedded structures based on guided waves.

Actually, leaky modes have often been considered for NDE in solid waveguides [2, 3, 4, 5, 6, 7], for which modes having low attenuation are desirable to maximise the inspection range. Analytical tools have been developed for modeling open elastic waveguides [8, 9] but they are limited to simple geometries (plates, cylinders).

For complex geometries, a classical approach relies on the finite element discretization of the eigenproblem in the transverse direction, which is often referred to as the Semi-Analytical Finite Element (SAFE) method (see for instance [10, 11, 12, 13]). Yet for open waveguides, one difficulty arises because the geometry is unbounded in the transverse directions. This difficulty is particularly severe due to the unusual behavior of leaky modes: while exponentially decreasing along the axis, leaky modes exponentially grow along the transverse directions. This phenomenon has been widely studied in electromagnetism (see [14, 15] for instance) and has sometimes been mentioned for elastodynamic waveguides [16, 17].

A simple procedure that can be used with existing codes has been proposed in [7, 18], which consists in using absorbing layers of artificially growing viscoelasticity. In practice, large layers may be required in order to reduce artificial reflections by the absorbing layer.

Instead of absorbing layers, an alternative approach to compute leaky modes is to use Perfectly Matched Layers (PML). Such a technique has already been applied to the scalar wave equation [19, 20] (i.e. acoustic, electromagnetic or SH waves). The goal of this work is to compute modes in open elastic waveguides by applying a SAFE-PML approach to the equations of elastodynamics (non-scalar). Theoretically, the PML technique allows to strongly attenuate any type of wave without reflection, thanks to an analytical continuation of equations into complex spatial coordinates. Compared to absorbing layers, one expects that the perfectly matched property will allow reduction of the artificial layer size. Another difference between the two approaches is seldom mentioned: computing leaky modes with PMLs is mathematically relevant, since both leaky modes and PMLs are defined through analytic extensions. On the contrary, the ability of absorbing viscoelastic layers to approximate leaky modes has, up to our knowledge, no theoretical explanation.

In this paper, one-dimensional modal problems are considered, i.e. bidimensional elastic waveguides corresponding to stratified planes. In Sec. 2, the SAFE-PML approach is presented. In Sec. 3, numerical solutions are validated thanks to analytical results of the literature. The efficiency of the perfectly matched technique is briefly compared to the absorbing layer method.

2 SAFE-PML method

2.1 Variational formulation

One assumes a linearly elastic material, small plane strains and displacements in the (x, z) plane. The time harmonic dependence is chosen as $e^{-i\omega t}$. z is the waveguide axis, x is the transverse direction. Acoustic sources and external forces are suppressed for the purpose of studying propagation modes.

The 2D variational formulation governing elastodynamics is given by:

$$\int_{\tilde{\Omega}} \delta\tilde{\boldsymbol{\epsilon}}^T \tilde{\boldsymbol{\sigma}} d\tilde{\Omega} - \omega^2 \int_{\tilde{\Omega}} \tilde{\rho}\delta\tilde{\mathbf{u}}^T \tilde{\mathbf{u}} d\tilde{\Omega} = 0 \tag{1}$$

where $d\tilde{\Omega} = d\tilde{x}dz$ (the tilde notation is explained in the next subsection). The variational formulation holds for any kinematically admissible trial displacement field $\delta\tilde{\mathbf{u}} = [\delta\tilde{u}_x\ \delta\tilde{u}_z]^T$. $\delta\tilde{\boldsymbol{\epsilon}}$ denotes the virtual strain vector $[\delta\tilde{\epsilon}_{xx}\ \delta\tilde{\epsilon}_{zz}\ \ 2\delta\tilde{\epsilon}_{xz}]^T$ and $\tilde{\boldsymbol{\sigma}}$ is the stress vector $[\tilde{\sigma}_{xx}\ \tilde{\sigma}_{zz}\ \tilde{\sigma}_{xz}]^T$. The superscript T denotes the matrix transpose. $\tilde{\rho}$ is the material density.

The stress-strain relationship is $\tilde{\boldsymbol{\sigma}} = \tilde{\mathbf{C}}\tilde{\boldsymbol{\epsilon}}$, where $\tilde{\mathbf{C}}$ is the matrix of material properties. If the material is isotropic, one has:

$$\tilde{\mathbf{C}} = \frac{E}{(1+\nu)(1-2\nu)} \begin{bmatrix} 1-\nu & \nu & 0 \\ \nu & 1-\nu & 0 \\ 0 & 0 & (1-2\nu)/2 \end{bmatrix} \tag{2}$$

where E is the Young modulus and ν denotes the Poisson coefficient.

Separating transverse from axial derivatives, the strain-displacement relation can be written as follows:

$$\tilde{\boldsymbol{\epsilon}} = (\mathbf{L}_{\tilde{x}} + \mathbf{L}_z \partial/\partial z)\tilde{\mathbf{u}} \tag{3}$$

where $\mathbf{L}_{\tilde{x}}$ is the operator containing all terms but derivatives with respect to the z-axis. For clarity, we have:

$$\mathbf{L}_{\tilde{x}} = \begin{bmatrix} \partial/\partial\tilde{x} & 0 \\ 0 & 0 \\ 0 & \partial/\partial\tilde{x} \end{bmatrix}, \quad \mathbf{L}_z = \begin{bmatrix} 0 & 0 \\ 0 & 1 \\ 1 & 0 \end{bmatrix} \tag{4}$$

2.2 Combining SAFE and PML

With a PML in the x direction, the formulation (1) can be interpreted as the analytical continuation of the equilibrium equations into the complex spatial coordinate $\tilde{x}$, with:

$$\tilde{x} = \int_0^x \gamma(\xi) d\xi \tag{5}$$

γ is a complex-valued function of x, satisfying:

- $\gamma(x)$=1 for $x \leqslant d$;
- $Im\{\gamma(x)\} > 0$ for $x > d$,

where $]d, \infty[$ must be understood as the exterior domain (the PML domain). In practice, the PML domain is truncated to $]d, d+h]$ with a closing boundary condition at $d+h$, arbitrarily chosen (usually of Dirichlet type).

From Eq. (5), the change of variables $\tilde{x} \mapsto x$ yields for any function $\tilde{f}$:

$$\frac{\partial \tilde{f}}{\partial \tilde{x}} = \frac{1}{\gamma}\frac{\partial f}{\partial x}, \quad d\tilde{x} = \gamma dx \tag{6}$$

where $\tilde{f}(\tilde{x}) = \tilde{f}(\tilde{x}(x)) = f(x)$.

In addition to the PML technique, the SAFE method is applied, which consists in applying an axial Fourier transform to the equilibrium equations. This is equivalent to assume an e^{ikz} dependence, where k is the axial wavenumber.

Combining SAFE and PML approach, the strain-displacement relation (3) becomes:

$$\boldsymbol{\epsilon} = \left(\frac{1}{\gamma}\mathbf{L}_x + ik\mathbf{L}_z\right)\mathbf{u} \tag{7}$$

where $\mathbf{L}_x$ is defined from Eq. (4) by replacing $\tilde{x}$ with x.

Finally, the FE discretization of the variation formulation (1) along the transverse direction x yields:

$$\{\mathbf{K}_1 - \omega^2\mathbf{M} + ik(\mathbf{K}_2 - \mathbf{K}_2^T) + k^2\mathbf{K}_3\}\mathbf{U} = \mathbf{0} \tag{8}$$

with the following elementary matrices:

$$\begin{array}{l} \mathbf{K}_1^e = \int_{x^e} \frac{1}{\gamma}\mathbf{N}^{eT}\mathbf{L}_x^T\mathbf{C}\mathbf{L}_x\mathbf{N}^e dx, \ \mathbf{K}_2^e = \int_{x^e} \mathbf{N}^{eT}\mathbf{L}_x^T\mathbf{C}\mathbf{L}_z\mathbf{N}^e dx, \\ \mathbf{K}_3^e = \int_{x^e} \gamma\mathbf{N}^{eT}\mathbf{L}_z^T\mathbf{C}\mathbf{L}_z\mathbf{N}^e dx, \ \mathbf{M}^e = \int_{x^e} \rho\gamma\mathbf{N}^{eT}\mathbf{N}^e dx \end{array} \tag{9}$$

where the column vector $\mathbf{U}$ contains nodal displacements and $\mathbf{N}^e$ is a matrix of nodal interpolating functions of displacement on the element.

Eq. (8) corresponds to an eigenvalue problem for the column vector $\mathbf{U}$ whose eigensolutions are the propagation modes. Note that the problem has been reduced from two dimensions to one dimension (from (x, z) to the transverse direction x of the waveguide).

Given ω and finding k, the eigenproblem is quadratic. The eigensystem can be linearized as:

$$(\mathbf{A} - k\mathbf{B})\hat{\mathbf{U}} = \mathbf{0} \tag{10}$$

with:

$$\mathbf{A} = \begin{bmatrix} \mathbf{0} & \mathbf{K}_1 - \omega^2\mathbf{M} \\ \mathbf{K}_1 - \omega^2\mathbf{M} & i(\mathbf{K}_2 - \mathbf{K}_2^T) \end{bmatrix} \tag{11}$$

and:

$$\mathbf{B} = \begin{bmatrix} \mathbf{K}_1 - \omega^2\mathbf{M} & \mathbf{0} \\ \mathbf{0} & -\mathbf{K}_3 \end{bmatrix}, \ \hat{\mathbf{U}} = \begin{Bmatrix} \mathbf{U} \\ k\mathbf{U} \end{Bmatrix} \tag{12}$$

This form corresponds to a generalized linear eigensystem that can be solved by numerical solvers. Yet due to the presence of the PML layer, $\mathbf{K}_1$, $\mathbf{K}_3$ and $\mathbf{M}$ are complex matrices and neither $\mathbf{A}$ nor $\mathbf{B}$ are Hermitian.

Thanks to the symmetry of $\mathbf{K}_1$, $\mathbf{K}_3$ and $\mathbf{M}$ and using the property $det\mathbf{D}^T = det\mathbf{D}$ ($\mathbf{D}$ is any matrix), it can easily be checked that if k is an eigenvalue of (8), then $-k$ is also an eigenvalue. Hence, the eigenproblem has two sets of eigensolutions $(k_j, \mathbf{U}_j^+)$ and $(-k_j, \mathbf{U}_j^-)$ $(j = 1, ..., n)$, representing n positive-going and n negative-going wave types (n being the number of degrees of freedom (dofs)).

2.3 PML function

The function $\gamma(x)$, user-defined and non-dimensional, must be responsible for wave attenuation inside the PML layer $]d, d+h]$. As recalled earlier, it must satisfy $Im\{\gamma\} > 0$ inside the layer ($x > d$) and $\gamma(x) = 1$ outside the PML (for $x \leqslant d$).

A constant function (i.e. $\gamma(x) = \bar{\gamma}$ where $\bar{\gamma}$ is a complex constant inside the PML) has generally been chosen when considering open waveguide problems [21, 19, 22]. This choice simplifies mathematical analysis of the problem.

However, the perfectly matched property ceases to exist due to the combined effects of discretization and truncature of the layer. As a consequence, it is desirable to have a rather slowly varying absorbing function $\gamma(x)$. Regardless waveguide analysis, several smooth functions have been proposed in the literature (see for instance [23, 24, 25]). One of the most popular is $\gamma(x) = 1 + i\sigma(x)/\omega$, where $\sigma(x)$ is an increasing quadratic function in the PML. $\gamma(x)$ here depends on the frequency.

In this paper, a parabolic function is proposed both for the real and imaginary parts of $\gamma(x)$. Any frequency dependence is dropped in order to avoid the computation of SAFE matrices at each frequency.

One defines $\bar{\gamma}$, the average value of γ in the PML:

$$\bar{\gamma} = \frac{1}{h}\int_d^{d+h} \gamma(s) ds \tag{13}$$

The parameter $\bar{\gamma}h$ can be readily interpreted. Let us denote k_x the transverse wavenumber for a given mode, obtained from the dispersion relation. From the interface to the end of the PML, wave fields are multiplied by $e^{ik_x\bar{\gamma}h}$, if the PML acts properly and reflection from the PML end is neglected. The argument of the exponential is complex and can be decomposed as follows:

$$e^{ik_x\bar{\gamma}h} = e^{i(Re(k_x)Re(\bar{\gamma}h) - Im(k_x)Im(\bar{\gamma}h))} e^{-(Re(k_x)Im(\bar{\gamma}h) + Im(k_x)Re(\bar{\gamma}h))} \tag{14}$$

Therefore for a given mode, the term $Re(k_x)Im(\overline{\gamma}h)+Im(k_x)Re(\overline{\gamma}h)$ represents the expected attenuation at the PML end, and the term $Re(k_x)Re(\overline{\gamma}h) - Im(k_x)Im(\overline{\gamma}h)$ represents the oscillating part of the wave. For leaky modes ($Re(k_x) > 0$ and $Im(k_x) < 0$), the attenuation is expected to increase if one increases $Im(\overline{\gamma})$ but decreases $Re(\overline{\gamma})$. For trapped modes ($Re(k_x) = 0$ and $Im(k_x) > 0$), the attenuation is expected to increase if we increase $Re(\overline{\gamma})$.

We could conclude that $Im(\overline{\gamma}h)$ should be high for a good approximation of leaky modes and $Re(\overline{\gamma}h)$ should be high for a good approximation of trapped modes. In practice, both leaky and trapped modes usually coexist, and we choose $Re(\overline{\gamma}h)$ with the same order of magnitude as $Im(\overline{\gamma}h)$.

It is also noted that $Re(\overline{\gamma}h)$ and $Im(\overline{\gamma}h)$ cannot be too high, otherwise the wavelength in the PML region becomes very small, which requires a finer mesh.

3 Results

Numerical tests are realized for three multilayer waveguides taken from the work of Lowe [8]. The first one is a three layer structure where only leaky modes are present, corresponding to a thin core of alpha case of 0.1mm embedded on both sides by titanium half-spaces. The second test case is a bilayer system, corresponding to a thin alpha case layer of 50 μm on titanium half-space. This case is of interest because the first mode is trapped in a low frequency range and becomes leaky mode at higher frequencies. The third case is also a bilayer system, an epoxy layer of 100 μm on aluminium half-space, for which the first two modes are trapped.

The longitudinal velocities c_l and shear velocities c_s of materials are respectively: 6060 and 3230 m/s (titanium), 6666 and 3553 m/s (alpha), 6370 and 3170 m/s (aluminium), 2610 and 1100 m/s (epoxy). Densities are: 4460 kg/m^3 (titanium, alpha), 2700 kg/m^3 (aluminium), and 1170 kg/m^3 (epoxy). These three cases will help to evaluate the efficiency of numerical methods on both trapped and leaky modes.

3.1 Preliminary remarks

As an example, the geometry of a bilayer waveguide is represented by Fig. 1. a is the core thickness, h is the thickness of the PML layer, d is the position of the PML interface.

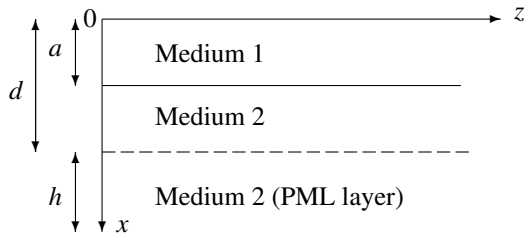

Figure 1: Geometry of a bilayer waveguide with PML in the transverse direction. With a SAFE method, only the x direction needs to be discretized.

Continuity of displacements and stresses is imposed at each interface, i.e., between the core and semi-infinite layers. In this paper, the thickness of PML layers is set to $0.9a$. Following the suggestion of [19, 26], the PML layer is close to the core ($d = 1.1a$) in order to reduce the effects of the exponential growth of leaky modes on the numerical results. A Dirichlet condition is chosen at the PML end (zero displacement). Finite elements are quadratic (three-node elements).

A difficulty is that the method will provide not only trapped and leaky modes, which are intrinsic to the physics of the problem, but also spurious modes which are resonating mainly in artificial layers and depend on the characteristics of these layers. Hence an important post-processing step consists in identifying and separating physical modes from unwanted modes. This step can be seen as modal filtering. The filtering criterion used for our tests is the ratio of kinetic energy in the PML region over the kinetic energy in the whole domain. Physical modes are then identified if this criterion is smaller than a user-defined value.

3.2 Validation

The reference solutions, taken from Lowe [8], are obtained from an analytical approach. SAFE dispersion curves are presented after modal filtering.

Let us first consider the three layer test case (titanium-alpha-titanium). Fig. 2 compares the results computed with γ constant and γ parabolic in the PML region, where $\overline{\gamma}h = 1+2i$ for both functions (h is kept constant). For conciseness, we only plot the imaginary part of the axial wavenumber (attenuation) as a function of frequency.

The parabolic function gives better results than the constant function. As already mentioned, this is explained by the fact that the PML method is no longer perfectly matched after discretization. Thus, the function γ should be chosen as smooth as possible to minimize reflection and obtain good simulation results. In the remainder, all PML results are obtained with γ parabolic.

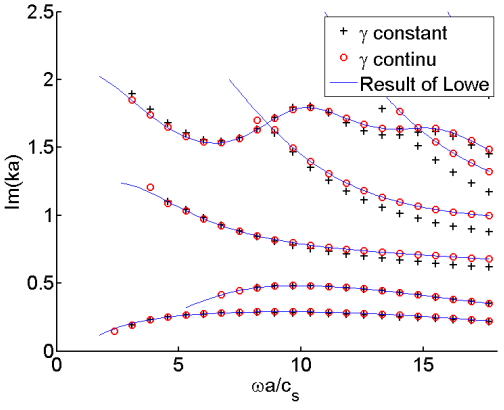

Figure 2: $Im(ka)$ vs. dimensionless frequency for titanium-alpha-titanium. Comparison between γ constant and parabolic.

Fig. 3 represents the attenuation as a function of frequency for the alpha-titanium bilayer ($\overline{\gamma}h = 4+4i$). Good agreement is obtained between the numerical results and those of Lowe. However, modes at low frequencies are filtered out due to insufficient attenuation by the PML. In fact, as the transverse wave number k_x is generally small for modes at low frequencies, the attenuating part of the term $e^{ik_x\overline{\gamma}h}$ becomes too small (non-negligible reflection occurs at the PML end). One remedy is to increase the PML thickness.

Fig. 4 gives a zoom on the less attenuated mode of Fig. 3. From the reference solution, it can be seen that this mode is trapped until a dimensionless frequency close to 4 is reached. When the mode is trapped, numerical results deviate from the reference curve. However the difference between simulation and reference is about 10^{-3} and numerical results are still acceptable. Those results can be improved by increasing $Re(\overline{\gamma}h)$ (see Sec. 2.3, results not shown for conciseness), or by increasing the PML thickness at low frequencies.

In conclusion, the SAFE-PML approach gives satisfying results both for leaky and trapped modes.

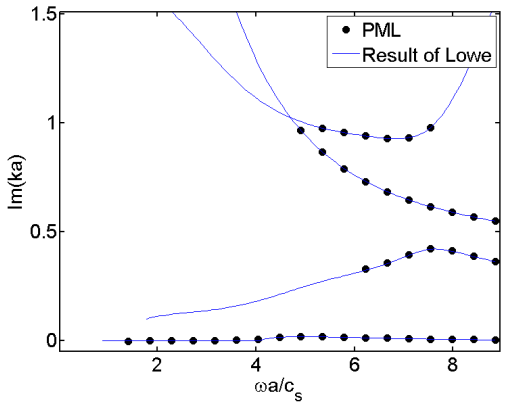

Figure 3: $Im(ka)$ vs. dimensionless frequency for alpha-titanium

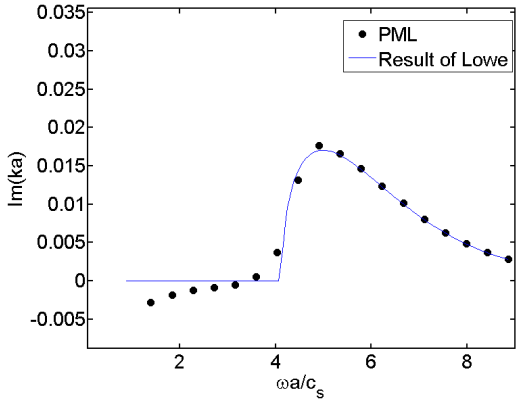

Figure 4: Same as Fig. 3. Zoom on the less attenuated mode.

3.3 Comparison with absorbing layers

Results obtained with PML are now compared with those obtained with absorbing layers in the case of the three-layer waveguide (titanium-alpha-titanium). The absorbing layer method consists in creating an artificial viscoelastic medium, the viscoelasticity growing smoothly in the transverse direction. Following [7, 18], elasticity coefficients are defined with an imaginary part cubically increasing, as follows:

$$\overline{C_{ij}} = \begin{cases} C_{ij}\left(1 - is\left(\frac{x-d_1}{h}\right)^3\right) & si \quad x < d_1 \\ C_{ij} & si \quad d_1 < x < d_2 \\ C_{ij}\left(1 - is\left(\frac{d_2-x}{h}\right)^3\right) & si \quad x > d_2 \end{cases} \qquad (15)$$

where d_1 and d_2 denote the interface positions of absorbing layers and s is a user-defined parameter. The thickness h of absorbing layers is set to $2.9a$, i.e. about three times larger than the PML thickness.

Fig. 5 compares the spectrum of $\lambda = -k^2$ at the dimensionless frequency $\omega a/c_s = 17.68$ obtained with PML and absorbing layers. Physical modes obtained by Lowe [8] (red triangles) are satisfyingly computed with both methods (though not clearly visible in Fig. 6, the results of Lowe are superimposed on numerical results, presented by black plus and blue circles). Because no modal filtering has been applied, one can observe that many other modes are indeed computed, as mentioned above.

With PML, such modes are located along two lines, both having equal rotation angles. The effect of PML has been thoroughly studied in [19, 26] for the scalar wave equation. By a direct analogy, one can interpret these modes as the discretisation of the continuous spectrum, whose rotation angle is $-2arg(\overline{\gamma})$ (about 116° here). With elastodynamics, the main difference lies in the fact that two branch cuts associated with longitudinal waves and shear waves occur instead of one with the scalar wave equation, which yields two continua.

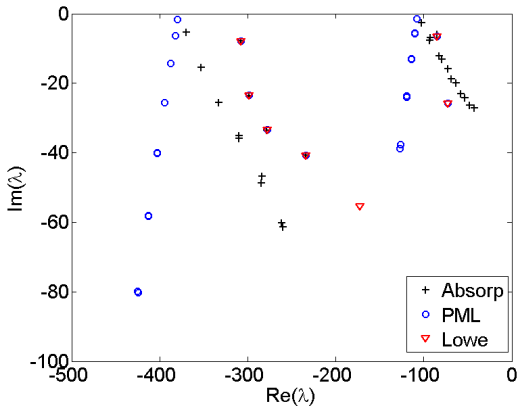

Figure 5: Spectrum of $\lambda = -k^2$ in the complex plane at $\omega a/c_s = 17.68$ (titanium-alpha-titanium).

Fig. 6 gives the spectrum at the dimensionless frequency $\omega a/c_s = 9.49$. One can observe that the PML method still performs well, while the absorbing layer technique fails at approximating physical modes. Surprisingly, attempts in optimizing the absorbing layer (by varying s and h) do not substantially improve these results. At this frequency, it seems that the transverse exponential growth of leaky modes is not sufficiently attenuated by the absorbing layers. This issue requires further research.

For trapped modes, the absorbing layers can yet give acceptable results, as shown by Fig. 7 representing the dispersion curve (phase velocity vs. frequency) for the epoxy-aluminium test case.

References

[1] R. N. Thurston. Elastic-waves in rods and clad rods. *Journal of the Acoustical Society of America*, 64(1):1–37.

[2] M. J. S. Lowe and P. Cawley. Comparison of the modal properties of a stiff layer embedded in a solid medium with the minima of the plane-wave reflection coefficient. *Journal of the Acoustical Society of America*, 97(3):1625–1637.

[3] M. J. S. Lowe and P. Cawley. The influence of the modal properties of a stiff layer embedded in a solid medium on the field generated in the

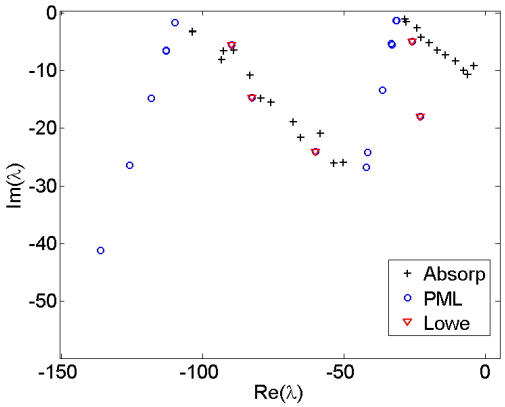

Figure 6: Same as Fig. 5 at $\omega a/c_s = 9.498$.

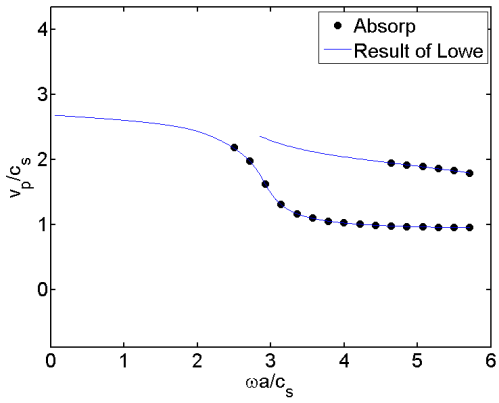

Figure 7: Dimensionless phase velocity v_p/c_s vs. frequency for epoxy-aluminium.

layer by a finite-sized transducer. *Journal of the Acoustical Society of America*, 97(3):1638–1649.

[4] M. D. Beard and M. J. S. Lowe. Non-destructive testing of rock bolts using guided ultrasonic waves. *International Journal of Rock Mechanics and Mining Sciences*, 40(4):527–536.

[5] M. D. Beard, M. J. S. Lowe, and P. Cawley. Ultrasonic guided waves for inspection of grouted tendons and bolts. *Journal of Materials in Civil Engineering*, 15(3):212–218.

[6] N. Ryden and M. J. S. Lowe. Guided wave propagation in three-layer pavement structures. *Journal of the Acoustical Society of America*, 116(5):2902–2913.

[7] M. Castaings and M. Lowe. Finite element model for waves guided along solid systems of arbitrary section coupled to infinite solid media. *Journal of the Acoustical Society of America*, 123(2):696–708.

[8] M. J. S. Lowe. *Plate waves for the NDT of diffusion bonded titanium*. PhD thesis, Mechanical Engineering Department, Imperial College London, 1992.

[9] B. Pavlakovic. *Leaky guided ultrasonic waves in NDT*. PhD thesis, Mechanical Engineering Department, Imperial College London, 1998.

[10] L. Gavric. Computation of propagative waves in free rail using a finite element technique. *Journal of Sound and Vibration*, 185:531–543, 1995.

[11] G. R. Liu and J. D. Achenbach. Strip element method to analyze wave scattering by cracks in anisotropic laminated plates. *Journal of Applied Mechanics*, 62:607–613, 1995.

[12] T. Hayashi, W.-J. Song, and J. L. Rose. Guided wave dispersion curves for a bar with an arbitrary cross-section, a rod and rail example. *Ultrasonics*, 41:175–183, 2003.

[13] I. Bartoli, A. Marzani, F. Lanza di Scalea, and E. Viola. Modeling wave propagation in damped waveguides of arbitrary cross-section. *Journal of Sound and Vibration*, 295:685–707, 2006.

[14] R. E. Collin. *Field Theory of Guided Waves*. IEEE Press, 1991.

[15] J. Hu and C. R. Menyuk. Understanding leaky modes: slab waveguide revisited. *Advances in Optics and Photonics*, 1:58–106, 2009.

[16] J. A. Simmons, E. Drescherkrasicka, and H. N. G. Wadley. Leaky axisymmetrical modes in infinite clad rods .1. *Journal of the Acoustical Society of America*, 92(2):1061–1090.

[17] A. C. Hladky-Hennion, P. Langlet, and M. de Billy. Conical radiating waves from immersed wedges. *Journal of the Acoustical Society of America*, 108(6):3079–3083.

[18] Z. Fan, M. J. S. Lowe, M. Castaings, and C. Bacon. Torsional waves propagation along a waveguide of arbitrary cross section immersed in a perfect fluid. *Journal of the Acoustical Society of America*, 124(4):2002–2010.

[19] A. S. Bonnet-BenDhia, B. Goursaud, C. Hazard, and A. Prieto. Finite element computation of leaky modes in stratified waveguides. In *5th Meeting of the Anglo-French-Research-Group*, volume 128, pages 73–86.

[20] A. S. Bonnet-BenDhia, B. Goursaud, C. Hazard, and A. Prieto. A multimodal method for non-uniform open waveguides. *International Congress on Ultrasonics, Proceedings*, 3(1):497–503.

[21] Y. Ould Agha, F. Zolla, A. Nicolet, and S. Guenneau. On the use of pml for the computation of leaky modes. an application to microstructured optical fibres. *The International Journal for Computation and Mathematics in Electrical and Electronic Engineering*, 27(1):95–109, 2008.

[22] A. Pelat, S. Felix, and V. Pagneux. A coupled modal-finite element method for the wave propagation modeling in irregular open waveguides. *Journal of the Acoustical Society of America*, 129(3):1240–1249.

[23] I. Harari and U. Albocher. Studies of fe/pml for exterior problems of time-harmonic elastic waves. *Computer Methods in Applied Mechanics and Engineering*, 195(29-32):3854–3879.

[24] F. Collino and C. Tsogka. Application of the perfectly matched absorbing layer model to the linear elastodynamic problem in anisotropic heterogeneous media. *Geophysics*, 66(1):294–307.

[25] A. Bermudez, L. Hervella-Nieto, A. Prieto, and R. Rodriguez. An optimal perfectly matched layer with unbounded absorbing function for time-harmonic acoustic scattering problems. *Journal of Computational Physics*, 223(2):469–488.

[26] B. Goursaud. *Étude mathématique et numérique de guides d'ondes ouverts non uniformes, par approche modale (Mathematical and numerical study of non uniform open waveguides, modal approach, in French)*. PhD thesis, École Polytechnique, 2010.